PNAS RESEARCH ARTICLE | IMMUNOLOGY AND INFLAMMATION

Augmenting antitumor efficacy of Th17-derived Th1 cells through IFN-γ-induced type I interferon response network via IRF7

Xiaoyi Lei[a,1], Ruipei Xiao[a,1], Zhe Chen[a,1], Jie Ren[a,1], Wenli Zhao[a], Wenting Tang[b], Kang Wen[c], Yihan Zhu[a], Xinru Li[a], Suidong Ouyang[d], Abai Xu[c,2], Yu Hu[b,2], and Enguang Bi[a,c,2]

Affiliations are included on p. 11.

Edited by George Stark, Cleveland Clinic Foundation, Cleveland, OH; received June 19, 2024; accepted October 14, 2024

The importance of CD4$^+$ T cells in cancer immunotherapy has gained increasing recognition. Particularly, a specific subset of CD4$^+$ T cells coexpressing the T helper type 1 (Th1) and Th17 markers has demonstrated remarkable antitumor potential. However, the underlying mechanisms governing the differentiation of these cells and their subsequent antitumor responses remain incompletely understood. Single-cell RNA sequencing (scRNA-seq) data reanalysis demonstrated the presence of $Th_{17}1$ cells within tumors. Subsequent trajectory analysis found that these $Th_{17}1$ cells are initially primed under Th17 conditions and then converted into IFN-γ-producing cells. Following the in vivo differentiation trajectory of $Th_{17}1$ cells, we successfully established in vitro $Th_{17}1$ cell culture. Transcriptomic profiling has unveiled a substantial resemblance between in vitro-generated $Th_{17}1$ cells and their tumor-infiltrating counterparts. $Th_{17}1$ cells exhibit more potent antitumor responses than Th1 or Th17 cells. Additionally, $Th_{17}1$chimeric antigen receptor T (CAR-T) cells eradicate solid tumors more efficiently. Importantly, $Th_{17}1$ cells display an early exhaustion phenotype while retaining stemness. Mechanistically, $Th_{17}1$ cells migrate faster and accumulate more in tumors in an extracellular matrix protein 1 (ECM1)-dependent manner. Furthermore, we show that IFN-γ up-regulated IRF7 to promote the type I interferon response network and ECM1 expression but decreased the exhaustion status in $Th_{17}1$ cells. Taken together, our findings position $Th_{17}1$ cells as a great candidate for improving targeted immunotherapies in solid malignancies.

T helper cells | adoptive cell transfer | type I interferon pathway | tumor immunotherapy | exhaustion

Significance

The limited efficacy of current T cell-based therapies against solid tumors often results from T cell exhaustion and inadequate tumor infiltration. Here, we identify a Th17-derived Th1 ($Th_{17}1$) subset coexpressing interferon gamma (IFN-γ) and interleukin-17 (IL-17) in the tumor microenvironment and establish the protocol to differentiate $Th_{17}1$ cells in vitro. $Th_{17}1$ cells have enhanced stemness, reduced exhaustion, and higher capability for tumor infiltration, probably driven by $Th_{17}1$ cell–derived IFN-γ and subsequent activation of interferon regulatory factor 7 (IRF7)-dependent type I interferon response. Accordingly, $Th_{17}1$ cells exhibit superior antitumor activity, revealing their potential to improve the efficacy of T cell-based therapies for solid tumors.

Adoptive T cell transfer (ACT) has demonstrated remarkable therapeutic efficacy in hematological patients, and extensive clinical research trials are being tested for solid tumors; however, limited effectiveness was achieved so far (1–3). One major obstacle is that the ex vivo expanded T cells are often terminal-differentiated and exhausted, primarily due to the high interleukin-2 (IL-2) concentration used for T cell expansion (3). Transferred cells tend to have a poor persistence after reinfusion (4). Therefore, scientists are actively exploring strategies to improve the quality and functionality of ex vivo expanded T cells to overcome this challenge (5, 6).

Novel techniques like single-cell RNA sequencing (scRNA-seq) have identified rare yet unique subsets of tumor-infiltrated T cells that are pivotal in clearing cancer cells (7–9). However, isolating these rare T cells or differentiating them ex vivo for use in ACT poses significant challenges. CD4$^+$ T cells have garnered increasing attention due to their ability to control tumor growth, both in immune checkpoint blockade and adoptive T cell therapy (7, 8, 10–13). Including to provide help to CD8$^+$ T cells, additional mechanisms for role of CD4$^+$ T cells have been illustrated that cytotoxic CD4$^+$ T cells can kill tumor directly in metastatic bladder cancer patients treated with anti-PD-L1 (14), or CD4$^+$ T cells toward a T helper type 1 (Th1)-directed phenotype induce inflammatory cell death for cancer cells (10). Among the major effector CD4$^+$ T cell subsets with antitumor function that can be readily detected in vivo, Th1 cells and Th17 cells stand out (15). Th1 cells highly express T-bet and IFN-γ, exhibit an impressive effector phenotype but are prone to apoptosis. Th17 cells highly express RORγt and IL-17 and display plasticity and preserved stemness, but their antitumor function remains controversial (15, 16). Atypical Th1 cells or hybrid Th1/Th17 cells, concurrently expressing IFN-γ and IL-17, have been documented in various human inflammatory autoimmune diseases and have also been validated in relevant mouse disease models (17–19). Notably, these hybrid Th1/Th17 cells have demonstrated heightened disease-associated potential. Furthermore, in vitro-differentiated Th1/Th17 cells have exhibited enhanced antitumor properties when transferred into tumor-bearing mice (19).

Author contributions: A.X., Y.H., and E.B. designed research; X.L., R.X., Z.C., J.R., W.Z., K.W., Y.Z., X.L., and E.B. performed research; W.T., K.W., and S.O. contributed new reagents/analytic tools; X.L., R.X., Z.C., and J.R. analyzed data; and X.L., R.X., Z.C., J.R., Y.H., and E.B. wrote the paper.

The authors declare no competing interest.

This article is a PNAS Direct Submission.

[1]X.L., R.X., Z.C., and J.R. contributed equally to this work.

[2]To whom correspondence may be addressed. Email: lc96xab@163.com, yuhu@smu.edu.cn, or bienguang1980@smu.edu.cn.

This article contains supporting information online at https://www.pnas.org/lookup/suppl/doi:10.1073/pnas.2412120121/-/DCSupplemental.

Published November 14, 2024.

However, the origins and functions of IFN-γ and IL-17 coexpressing T cells within the tumor microenvironment remain elusive, and the underlying mechanisms responsible for their superior antitumor functionality need further investigation.

In this study, we reported the presence of a Th17-derived Th1 subset (referred to as $Th_{17}1$) within tumors, which shows a positive correlation with the survival status of cancer patients. Following the in vivo differentiation trajectory of $Th_{17}1$ cells, we successfully cultured $Th_{17}1$ cells in vitro and found that in vitro generated $Th_{17}1$ cells closely resemble the gene signature and functional pathways of tumor-infiltrated $Th_{17}1$ cells. $Th_{17}1$ cells and $Th_{17}1$ CAR-T cells demonstrate superior antitumor function with a less exhausted phenotype. ECM1 is highly expressed in $Th_{17}1$ cells, endowing $Th_{17}1$ cells with better migration to the tumor and superior antitumor efficacy. Furthermore, we provide evidence that IFN-γ-induced IRF7 is required for the low exhausted status and increased expression of ECM1 in $Th_{17}1$ cells.

Results

Presence and Implication of IL-17$^+$IFN-γ$^+$ Cells in the Tumor Microenvironment. To gain insights into the subsets of CD4$^+$ helper cells in the tumor microenvironment, we reanalyzed the pan-T cell scRNA-seq data published by Zhang et al. (9). We segregated 18 distinct cell clusters, with 16 of these clusters delineated as various CD4$^+$ T cell subsets, including pre-exhausted, proliferating, resident memory, Th1-like effector, Th17, and Treg cells, by uniform manifold approximation and projection (UMAP) clustering via Seurat (*SI Appendix*, Fig. S1 *A* and *B*). However, clusters 3 and 10 posed a challenge in conventional classification due to coexpression of markers associated with both Th1 and Th17 phenotypes (*SI Appendix*, Fig. S1*B*). Remarkably, the colocalization of key Th1 and Th17 markers, *IL17A* and *IFNG* (Fig. 1*A*), unveiled a distinct subset termed $Th_{17}1$ cells (Fig. 1*B* and *SI Appendix*, Fig. S1*B*), constituting approximately 13% of the total CD4$^+$ T cells (Fig. 1*B*). This specific subset exhibited simultaneous expression of Th1 marker genes (*IFNG* and *TBX21*) and Th17 signature genes (*RORC* and *IL17A*), confirmed by Dotplot analysis in Seurat (Fig. 1*C*). Pathway analysis using Gene Set Variation Analysis (GSVA) showed an upregulation of memory and effector-related pathways in $Th_{17}1$ cells, contrasting with down-regulated dysfunctional and Treg-associated pathways (Fig. 1*D*). Intriguingly, pseudotime and trajectory analysis disclosed that Th17 cells could differentiate into both Th1 and $Th_{17}1$ subsets independently, underscoring the uniqueness of $Th_{17}1$ cells as a separate entity (Fig. 1*E*). Additionally, BEAM mapping identified distinctive genes associated with $Th_{17}1$ differentiation (*SI Appendix*, Fig. S1*C*). To explore the clinical relevance, we conducted pancancer Kaplan–Meier survival analysis. Patients exhibiting high Th1, Th17, and $Th_{17}1$ signatures all displayed improved overall survival compared to their low signature counterparts (Fig. 1*F*). Notably, patients with high $Th_{17}1$ signatures displayed the most favorable 5-y (*SI Appendix*, Fig. S1*D*) and 10-y (Fig. 1*F*) overall survival rates compared to those with high Th1 or high Th17 signatures. To determine whether $Th_{17}1$ cells originate from Th17 cells in the tumor microenvironment, we utilized IL-17 reporter mice as previously reported (20). Naive CD4$^+$ T cells from OTII CD45.1$^+$ IL-17 reporter mice were differentiated into Th17 cells in vitro. GFP$^+$ Th17 cells were then sorted (Fig. 1*G*) and transferred into C57BL/6 mice bearing MB49-OVA tumors. Five days posttransfer, $Th_{17}1$ cells were readily detected in tumors but were rare in the spleen. Additionally, $Th_{17}1$ cells originating from endogenous CD4$^+$ T cells were scarcely detected in this tumor model (Fig. 1 *H* and *I*). Consequently, we defined the $Th_{17}1$ subset within the tumor microenvironment as an entity that is positively correlated with patient survival.

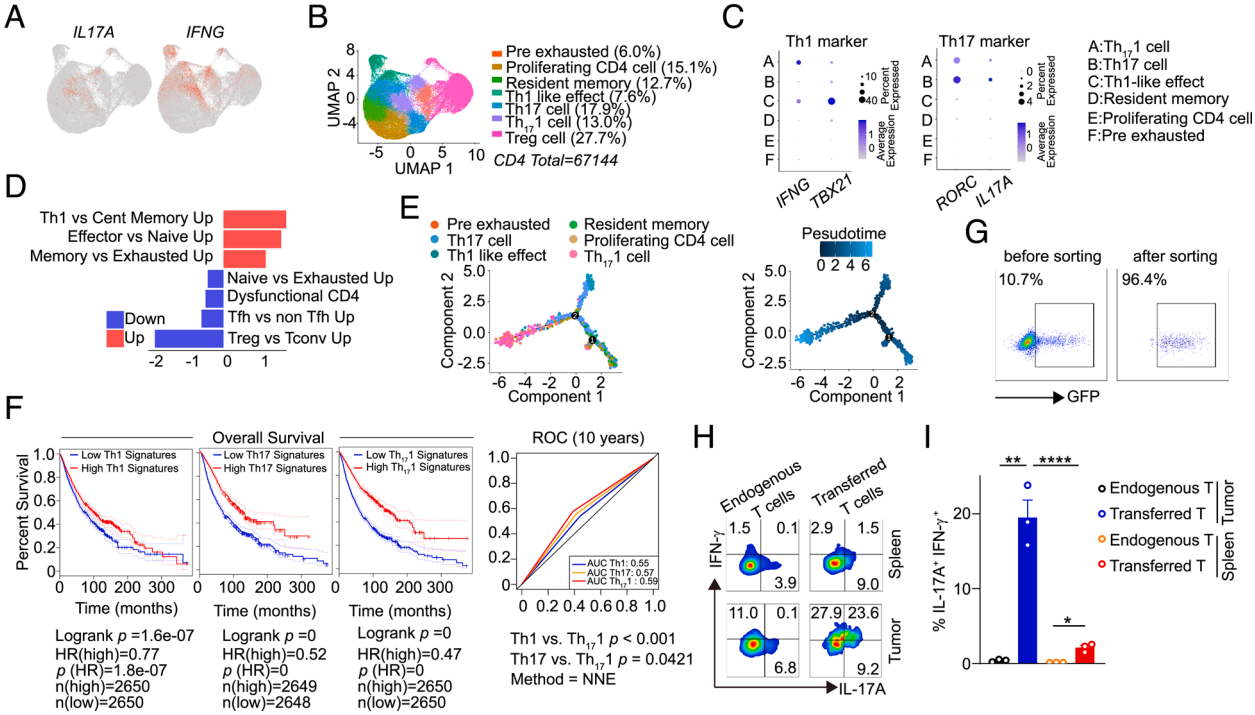

Fig. 1. IL-17$^+$IFN-γ$^+$ cells are present in tumor microenvironment and positively correlated with patient survival. (*A*) Feature plot shows coexpression of IL-17 and IFN-γ in tumor-infiltrating CD4$^+$ T cells. (*B*) Annotation of cell types for distinct groups. (*C*) Marker specificity for Th1 and Th17 cells shown in a dot plot. (*D*) GSVA of pathway alterations in $Th_{17}1$ cells compared to other cell types. (*E*) Pseudotemporal analysis showing evolutionary trajectory of tumor-infiltrating CD4$^+$ T Cells. (*F*) Kaplan–Meier survival analysis and ROC curves showing prognostic performance of Th1, Th17, and $Th_{17}1$ signatures across cancers. AUC (Area Under the ROC Curve). (*G*) Percentage of GFP$^+$ Th17 cells from CD45.1$^+$ OTII IL-17 reporter mice before and after sorting. (*H* and *I*) Flow cytometry analysis of IFN-γ and IL-17A in CD45.1$^+$ OTII IL-17 reporter Th17 cells 5 d posttransfer in both the spleen and tumor from MB49-OVA tumor-bearing mice. Data are presented as mean ± SEM. **P* < 0.05; ***P* < 0.01; *****P* < 0.0001.

In Vitro-Differentiated $Th_{17}1$ Cells Resemble Intratumor IL-17$^+$IFN-γ$^+$ $Th_{17}1$ Subset. While atypical Th1 cells coexpressing IFN-γ and IL-17 under Th1 and Th17 mixed culture condition have been reported (19), investigation of $Th_{17}1$ cells remains unexplored. Mimicking the differentiation trajectory of tumor-infiltrating $Th_{17}1$ cells, we developed a procedure for in vitro differentiation of $Th_{17}1$ cells (Fig. 2*A*), alongside categorization of other subsets as Th1-derived Th1 (Th1), Th1-derived Th17 ($Th_1$17), and Th17-derived Th17 (Th17). Morphologically, Th1, Th17, and $Th_{17}1$ cells exhibited similar cell size (*SI Appendix*, Fig. S2*A*), while Th17 cells displayed slower growth kinetics compared to the other subsets (*SI Appendix*, Fig. S2*B*). In vitro differentiated $Th_{17}1$ cells were able to produce both IFN-γ and IL-17A but not Th1, $Th_1$17, and Th17 cells (Fig. 2*B* and *SI Appendix*, Fig. S2*C*). To assess the similarity between in vitro differentiated and tumor-infiltrating $Th_{17}1$ cells, we performed bulk RNA-seq for in vitro-differentiated Th1, Th17, and $Th_{17}1$ cells on day 9 (Fig. 2*A*). Using the universal markers of T cell subsets, we revealed a mixed Th1 and Th17 signature akin to that of in vivo $Th_{17}1$ cells (Fig. 2*C*). Comparison of genes captured in both bulk RNA-seq and scRNA-seq datasets highlighted a set of unique genes specific to in vitro-differentiated $Th_{17}1$ cells (*SI Appendix*, Fig. S3*A*), exhibiting a trend of transcriptomic resemblance to their in vivo counterparts. Further analysis identified 84 up-regulated and 27 down-regulated genes unique to $Th_{17}1$ cells, surpassing those in Th1 and Th17 cells, with similar trends observed in the scRNA-seq dataset (56 up-regulated and 14 down-regulated genes, *SI Appendix*, Table S1). Utilizing the expression pattern of these genes, we demonstrated the closeness of $Th_{17}1$ cells to tumor-infiltrating $Th_{17}1$ cells (*SI Appendix*, Fig. S3*B*). Functional correlation analysis via GSVA revealed broad similarity between in vitro and in vivo $Th_{17}1$ cells in critical T cell pathways (*SI Appendix*, Fig. S3*C*), including activation, differentiation, metabolism, and response to metal ion (21–26). Moreover, the $Th_{17}1$ signature positively correlated with patient overall survival (Fig. 1*F*), prompting an investigation into whether the in vitro-derived $Th_{17}1$ cell signature exhibited similar prognostic value. Among the 84 up-regulated genes in $Th_{17}1$ cells, 41 were found to be CD4-related in The Cancer Genome Atlas (TCGA) data (*SI Appendix*, Fig. S3*D* and Table S2). When we reflected the in vitro-differentiated $Th_{17}1$ cells using these signature genes into the UMAP of tumor-infiltrated CD4$^+$ T cell subsets in pancancer patients, the in vitro-differentiated $Th_{17}1$ cells match the in vivo $Th_{17}1$ cells very well (Fig. 2*D*). This gene set was used for survival analysis in TCGA data encompassing various tumor types (BLCA, BRCA, CESC, HNSC, LIHC, LUAD, OV, COAD), revealing a positive correlation between high scores of this gene set and favorable prognosis (Fig. 2*E*). Overall, our findings underscore the likeness between in vitro-differentiated $Th_{17}1$ cells and tumor-infiltrated $Th_{17}1$ cells across gene expression, functional pathways, and patient survival correlation.

$Th_{17}1$ Cells Demonstrate Superior In Vivo Antitumor Efficacy. To evaluate the antitumor efficacy of in vitro-differentiated $Th_{17}1$ cells, B16-OVA lung metastasis model was first employed because the model is very sensitive to treatment. $Th_{17}1$ cells have robust antitumor potential, evidenced by reduced tumor foci, tumor weight, and lung tissue weight compared to Th1 and Th17 cell (Fig. 3 *A* and *B* and *SI Appendix*, Fig. S4*A*).

To investigate the antitumor efficacy of $Th_{17}1$ cells on solid tumor, a C57BL/6 mice model bearing B16-OVA solid tumors was employed. $Th_{17}1$ cells exhibited potent tumor control ability resulting in smaller tumor sizes and prolonged survival rates compared to Th1 and Th17 cells (Fig. 3*C* and *SI Appendix*, Fig. S4*B*). Here, we found Th1 cells have almost no tumor-controlling function probably due to the repeated stimulation and overtime culture in vitro. Analysis of T cell dynamics in the blood showed that $Th_{17}1$ cells were the most abundant on day 5 posttransfer (Fig. 3 *D* and *E*). Additionally, $Th_{17}1$ cells demonstrated superior in vivo persistence, showing a slight increase in their numbers (Fig. 3 *D* and *E*). This trend was consistent with the higher presence of tumor-infiltrating $Th_{17}1$ cells compared to Th1 and Th17 cells on day 15 (Fig. 3*F* and *SI Appendix*, Fig. S4*C*). Further investigation into CD8$^+$ T cells in the blood revealed intriguing dynamics, with $Th_{17}1$-treated mice exhibiting sustained levels of CD8$^+$ T cells compared to Th1 and Th17 group (Fig. 3*G* and *SI Appendix*, Fig. S4*D*). Moreover, CD44$^+$ CD8$^+$ T cell proportions were significantly higher in tumors treated with $Th_{17}1$ cells (*SI Appendix*, Fig. S4 *E* and *F*). Interestingly, depletion of CD8$^+$ T cells significantly impaired the antitumor function of $Th_{17}1$ but not Th1 and Th17 cells (Fig. 3*H* and *SI Appendix*, Fig. S4*G*), underscoring their unique mechanism of action.

Finally, we assessed the clinical translational potential of $Th_{17}1$ cells in CAR-T immunotherapy using the MB49-CD19 tumor model, comparing their efficacy to that of Th17 CAR-T cells. $Th_{17}1$ CAR-T cells demonstrated significant inhibition of tumor growth and prolonged mouse survival (Fig. 3 *I* and *J*). After being cultured for 10 d in vitro, $Th_{17}1$ CAR-T cells exhibited significantly lower PD-1 expression compared to Th17 CAR-T cells prior to T cell transfer (Fig. 3*K* and *SI Appendix*, Fig. S4*H*). Following transfer, PD-1 expression in $Th_{17}1$ CAR-T cells increased to levels similar to those of Th17 CAR-T cells, possibly indicating reactivation in vivo. However, on days 14 and 21, PD-1 expression in $Th_{17}1$ CAR-T cells was substantially lower, suggesting a less exhausted phenotype (Fig. 3*K* and *SI Appendix*, Fig. S4*H*). Consistently, Th17 CAR-T cells exhibited a faster decrease and became undetectable on day 21 in the blood, whereas approximately 20% of CAR-T cells persisted in the $Th_{17}1$ group, possibly due to their less exhausted nature (Fig. 3*L*). Furthermore, $Th_{17}1$ CAR-T cells were significantly more abundant in tumors (Fig. 3*M*).

$Th_{17}1$ Cells Exhibit Intermediate Apoptotic and Metabolic Characteristics. Th1 cells have potent cytotoxicity, however, their susceptibility to apoptosis curtails the in vivo therapeutic efficacy (27). Genes regulating positive leukocyte apoptotic processes were intermediately enriched by gene set enrichment analysis (GSEA) of in vitro-cultured $Th_{17}1$ cells compared to Th1 and Th17 cells (*SI Appendix*, Fig. S5 *A* and *B*), which is consistent with the Annexin V and PI staining (*SI Appendix*, Fig. S5*C*). High level of the antiapoptotic protein Bcl-2 was observed in $Th_{17}1$ cells, akin to Th17 cells (*SI Appendix*, Fig. S5*D*). Metabolic status profoundly influences T cell function and survival within the tumor microenvironment (28). $Th_{17}1$ cells exhibited intermediate oxidative phosphorylation marked by mitochondrial oxygen consumption rate (*SI Appendix*, Fig. S5*E*). Basal respiration, maximal respiration, and adenosine triphosphate production were likewise intermediate in $Th_{17}1$ cells, indicating their metabolic state (*SI Appendix*, Fig. S5*F*). Intriguingly, in the B16-OVA solid tumor model, tumor-infiltrating OTII $Th_{17}1$ cells exhibited the highest mitochondrial mass among these three subsets detected by flow cytometry (*SI Appendix*, Fig. S5*G*).

$Th_{17}1$ Cells Display Early Exhausted Phenotype with Stemness. T cell exhaustion is characterized by reduced effector function and persistence, leading to uncontrolled cancer growth (29). Using a four-stage exhaustion model to analyze our RNA-seq data (30), we found that progenitor 1 exhaustion (stage 1) signature genes were enriched in $Th_{17}1$ cells, progenitor 2 exhaustion (stage 2) signature genes were highly expressed in Th17 cells, and intermediate and terminal exhausted signatures (stage 3 and stage 4) were displayed

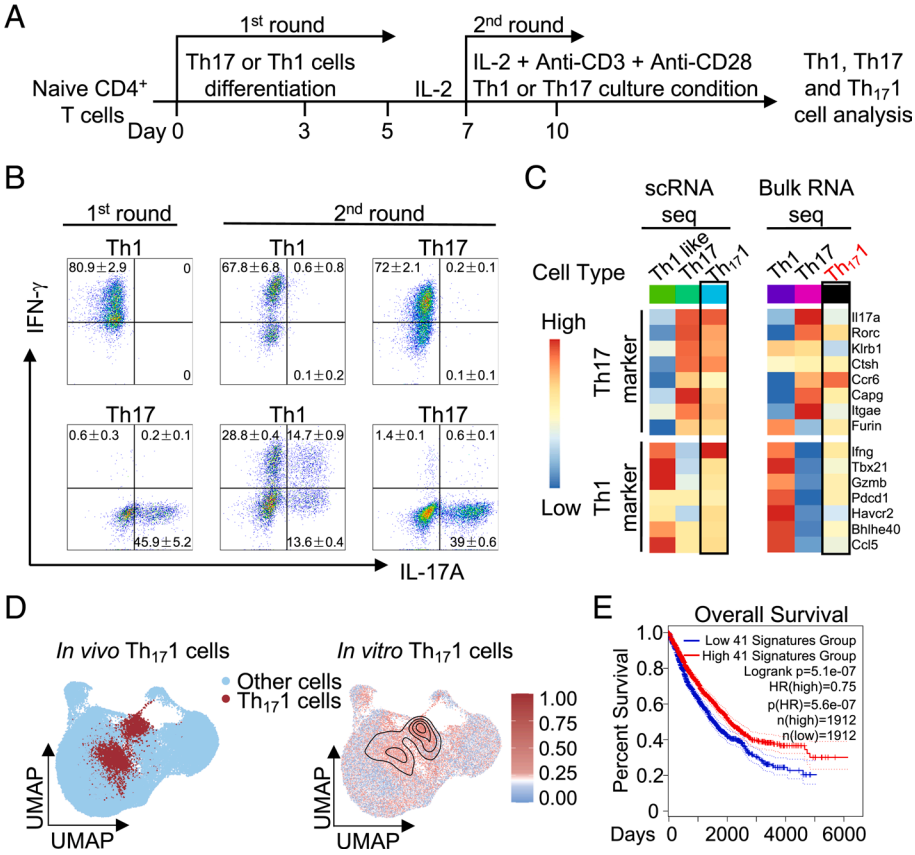

Fig. 2. $Th_{17}1$ cells mimic the intratumor IL-17$^+$IFN-γ$^+$ subsets. (*A*) A schematic diagram depicts the experimental design for $Th_{17}1$ cell differentiation in vitro. (*B*) Flow cytometry showing IL-17 and IFN-γ expression in cells from first and second differentiation rounds on days 3 and 9. (*C*) Comparison of intratumoral scRNA-seq data of IL-17$^+$IFN-γ$^+$ subsets (9) with our bulk RNA-seq transcriptional profiles of Th1, Th17, and $Th_{17}1$ cells differentiated in vitro by universal Th1 and Th17 markers. (*D*) UMAP of in vivo $Th_{17}1$ cells from pan-cancer patients and the reflection of in vitro-differentiated $Th_{17}1$ cells by the 41 genes set. (*E*) Kaplan–Meier survival analysis based on high or low expression of the 41-gene $Th_{17}1$ signature. Experiments shown in *B* were performed with three biological replicates. Data are presented as mean ± SEM. ****$P < 0.0001$.

in Th1 cells (Fig. 4*A* and *SI Appendix*, Table S3). These results demonstrated that $Th_{17}1$ cells are less exhausted. Flow cytometry analysis of Ly108 and CD69 expression further validated that $Th_{17}1$ cells were less in the terminal exhaustion status (stage 3/4) (Fig. 4 *B*–*D*) (30), highlighting the less exhausted phenotype of $Th_{17}1$ cells. Upon transfer into B16-OVA-bearing mice, $Th_{17}1$ cells maintained their less exhaustion phenotype on day 5 post transfer (Fig. 4 *E* and *F*). As time progressed, both $Th_{17}1$ and Th17 cells transitioned toward stages 1 and 2 exhaustion, while Th1 cells increasingly exhibited late-stage exhaustion in the blood of mice (Fig. 4*F*). Additionally, splenic $Th_{17}1$ cells showed an earlier exhaustion feature (Fig. 4 *G* and *H*). In vitro-cultured $Th_{17}1$ cells expressed moderate levels of exhaustion markers PD-1 and LAG-3 (Fig. 4*I*). These findings indicated that $Th_{17}1$ cells maintained an early exhaustion phenotype. Features for progenitor exhausted T cells include self-renewal, prolonged proliferation, differentiation capabilities, and signifying "stemness" (30). We noticed an upregulation of stemness-associated genes in $Th_{17}1$ cells, including *Slamf6*, *Il2rg*, *Myb*, and *Id3* by RNA-seq (Fig. 4*J*), and *Il2rg*, *Myb,* and *Sell* by qPCR (Fig. 4*K*).

ECM1 Drives Enhanced Migration and Antitumor Function of $Th_{17}1$ Cells. To elucidate the mechanism behind the heightened antitumor potency of $Th_{17}1$ cells, we analyzed the RNA-seq data employing CBNplot, a Bayesian network diagram approach for enrichment analysis (31). One of the enriched gene regulatory networks (GRN) is the migration-related pathways in $Th_{17}1$ cells (Fig. 5*A*). Furthermore, GSVA of the scRNA-seq data (9) also showed elevated Z scores for cell adhesion and migration pathways in tumor-infiltrating $Th_{17}1$ cells (Fig. 5*B*). Given the importance of efficient migration into solid tumors for successful ACT and the significantly increased abundance of $Th_{17}1$ abundance in solid tumors (Fig. 3*F*), we next evaluated the migration abilities of $Th_{17}1$ cells. Transwell assays demonstrated significantly better migration ability of $Th_{17}1$ cells (Fig. 5 *C* and *D*).

Based on transcriptomic analysis, we found $Th_{17}1$ cells have a higher expression of *Ecm1* (Fig. 5*E*), which has been identified as a crucial driver of T cell migration (32). We further verified ECM1 expression pattern from mRNA (Fig. 5*F*) and protein levels (Fig. 5*G*).

To ascertain the function of ECM1 in enhancing $Th_{17}1$ cells' migratory capacity, we employed ECM1 knockout (KO) mice to generate $Th_{17}1$ cells. ECM1 deficiency did not affect $Th_{17}1$ CAR-T cells' size (*SI Appendix*, Fig. S6*A*). Strikingly, the migration potential of $Th_{17}1$ cells was severely impaired when ECM1 is lacking, suggesting a pivotal role of ECM1 in facilitating $Th_{17}1$ cell migration (Fig. 5 *H* and *I*). To further establish whether $Th_{17}1$ cells exert their superior antitumor ability through an ECM1-dependent mechanism, we employed wild-type (WT) or ECM1 KO $Th_{17}1$ CAR-T cells to treat MB49-CD19 bladder tumors (Fig. 5*J*). Consistently, WT $Th_{17}1$ CAR-T cells effectively controlled tumor growth, whereas ECM1 KO $Th_{17}1$ CAR-T cells exhibited compromised antitumor function (Fig. 5*J*), with corresponding results observed in mouse survival (Fig. 5*K*). To assess whether ECM1 deficiency affects CAR-T cell migration in vivo, we analyzed CAR-T cells in CAR-T treated tumor-bearing mice on day 7 post T cell transfer. ECM1 deficiency did not decrease cell numbers in the mouse spleen (*SI Appendix*, Fig. S6*B*), but resulted in a dramatic decrease in cell

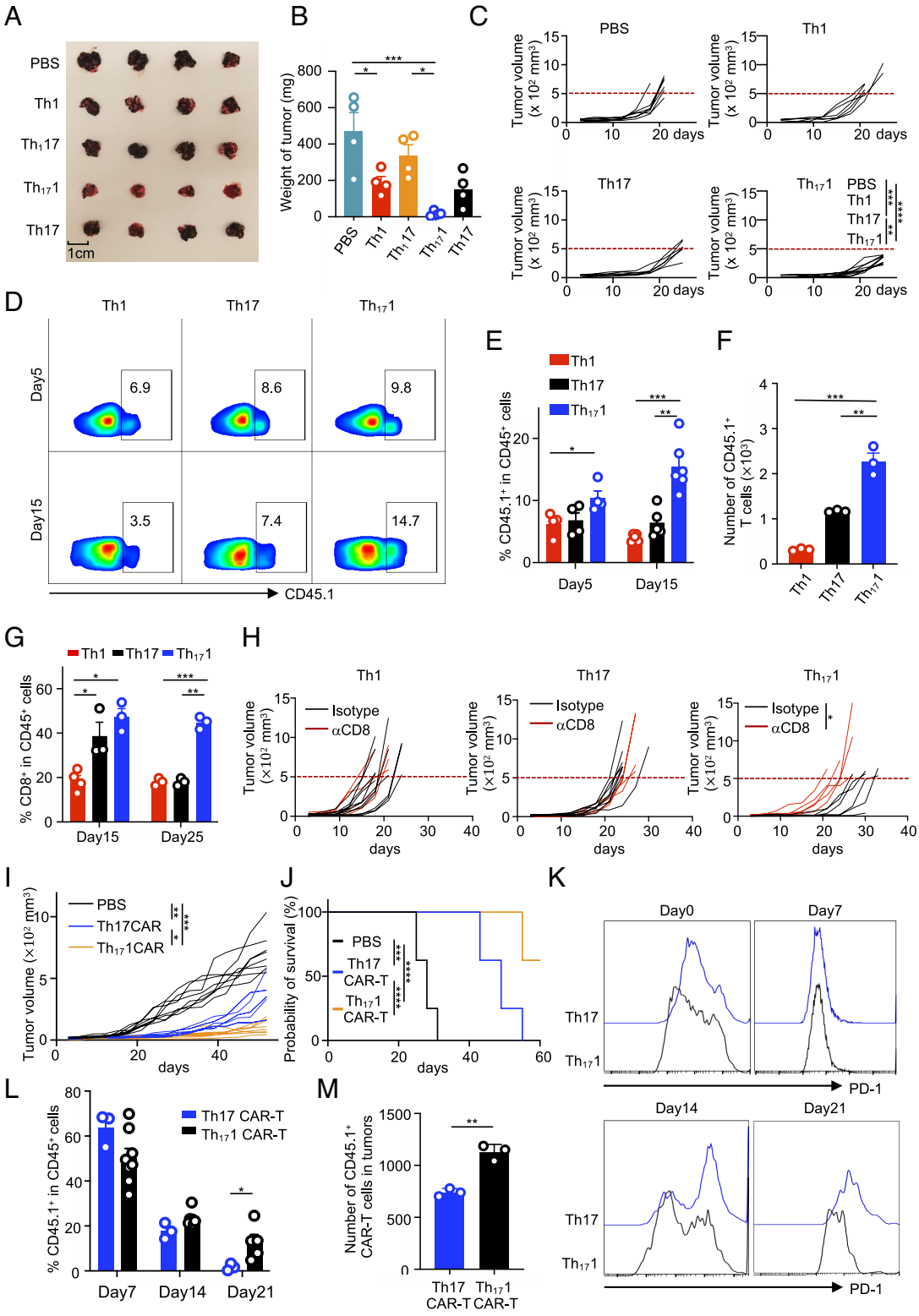

Fig. 3. $Th_{17}1$ cells possess the best antitumor effect. (*A* and *B*) C57BL/6 mice were intravenously injected with B16-OVA cells and CD45.1$^+$ OTII Th1, Th17, $Th_{17}17$, and $Th_{17}1$ cells (cultured for 10 d in vitro). Lung images show tumor burden in different treatment groups (*A*) and tumor weight measurements (*B*) (n = 4). (*C*–*H*) Mice with subcutaneous B16-OVA tumors were treated with CD45.1$^+$ OTII Th1, Th17, or $Th_{17}1$ cells on day 5. (*C*) Tumor growth curves are shown (n = 6 to 10). Percentages of donor T cells in blood (*D* and *E*) and tumors (*F*), endogenous CD8$^+$ T cells in blood (*G*) on indicated days. (*H*) Tumor growth in the B16-OVA model treated with isotype or CD8 antibody (n = 4 to 6). (*I*–*M*) CAR-T cell treatment in tumor model. Tumor growth (*I*) and survival (*J*) curves for Th17 and $Th_{17}1$ CAR-T cells (n = 8 to 10). PD-1 expression in CAR-T cells in vitro and in vivo (*K*), CAR-T cells in blood (*L*), and tumor (*M*). Data are from independent experiments (*A*, *C*, and *H*) and single experiment (*H*). Data are presented as mean ± SEM. *$P < 0.05$; **$P < 0.01$; ***$P < 0.001$; ****$P < 0.0001$.

migration into draining lymph nodes (*SI Appendix*, Fig. S6*C*) and tumors (Fig. 5*L*). Moreover, the persistence of KO $Th_{17}1$ CAR-T cells in the circulation was notably diminished compared to their WT counterparts on day 14 after T cell transfer (Fig. 5*M*). Collectively, these results indicated that ECM1 is key for the heightened migration and enhanced antitumor activity in $Th_{17}1$ cells.

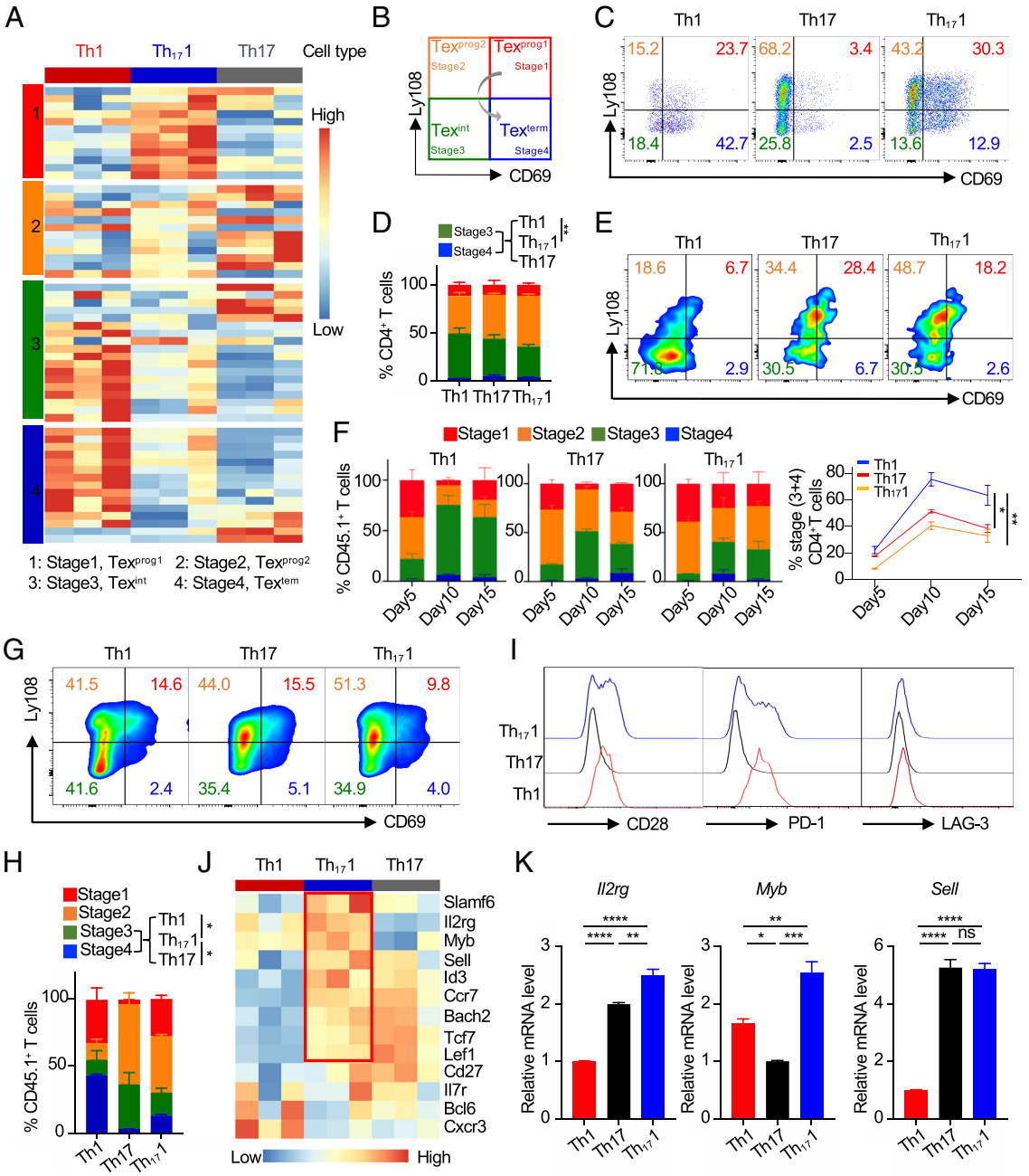

Fig. 4. $Th_{17}1$ cells exhibit early exhausted phenotype and better stemness. (*A*) Heatmap comparing exhaustion stage-specific genes (*SI Appendix*, Table S3) in RNA-seq data from in vitro-differentiated Th1, Th17, and $Th_{17}1$ cells. (*B*) Diagram of T cell exhaustion progression across four stages. (*C* and *D*) Flow cytometry analysis of CD69 and Ly108 expression on in vitro-differentiated Th1, Th17, and $Th_{17}1$ cells on day 10. (*E* and *F*) Exhaustion stages of transferred Th1, Th17, and $Th_{17}1$ cells in the blood of B16-OVA tumor-bearing mice on days 5, 10, and 15 posttransfer (n = 3). (*G* and *H*) CD69 and Ly108 expression on transferred cells in the spleen on day 10. (*I*) CD28, PD-1, and LAG-3 expression on in vitro-differentiated cells on day 11. (*J*) Heatmap showing stemness marker expression in Th1, Th17, and $Th_{17}1$ cells. (*K*) qPCR analysis of *Il2rg*, *Myb*, and *Sell* expression. Data are representative of at least two independent experiments except RNA-seq data. Data are presented as mean ± SEM. **P* < 0.05; ***P* < 0.01; ****P* < 0.001; *****P* < 0.0001.

IRF7 Confers $Th_{17}1$ Cells with a Unique Type I IFN Response Transcriptome and Orchestrates the Early Exhausted Phenotype and ECM1 Upregulation. Another inferred GRN is the network of the response to type I interferon in $Th_{17}1$ cells (Fig. 5*A*), which is also enriched by GSVA of scRNA-seq data (Fig. 5*B*). Type I IFN signaling has been linked to both $CD8^+$ T cell exhaustion (33) and reduced exhaustion in specific $CD4^+$ T cell subsets (34). We explored the relationship between this pathway and the exhaustion status of $Th_{17}1$ cells. GSEA demonstrated an increased type I interferon-mediated signaling pathway in $Th_{17}1$ cells compared to Th1 and Th17 cells (Fig. 6*A*), supported by the expression of type I IFN signature genes, including Stat and type I interferon-stimulated genes (ISGs) (Fig. 6*B*). RNA-seq data revealed a unique set of transcription factors in $Th_{17}1$ cells, in which *Irf7*, *Stat1*, and *Stat2* are closely related with type I IFN pathway (*SI Appendix*, Fig. S7*A*). Further analysis of the up-regulated genes in $Th_{17}1$ cells using protein–protein interaction (PPI) network suggested a central role of IRF7 (Fig. 6*C*), which is highly expressed in $Th_{17}1$ cells (Fig. 6*D*). Since IRF7 is the master regulator of type I interferon responses (35), the intriguing question was whether IRF7-dominant type I interferon signature was required for the unique phenotype in $Th_{17}1$ cells. Knockdown of IRF7 reduced the expression of ISG genes such as *Isg15*, *Oasl2*, and *Mx1* (*SI Appendix*, Fig. S7 *B–E*), and led to increased

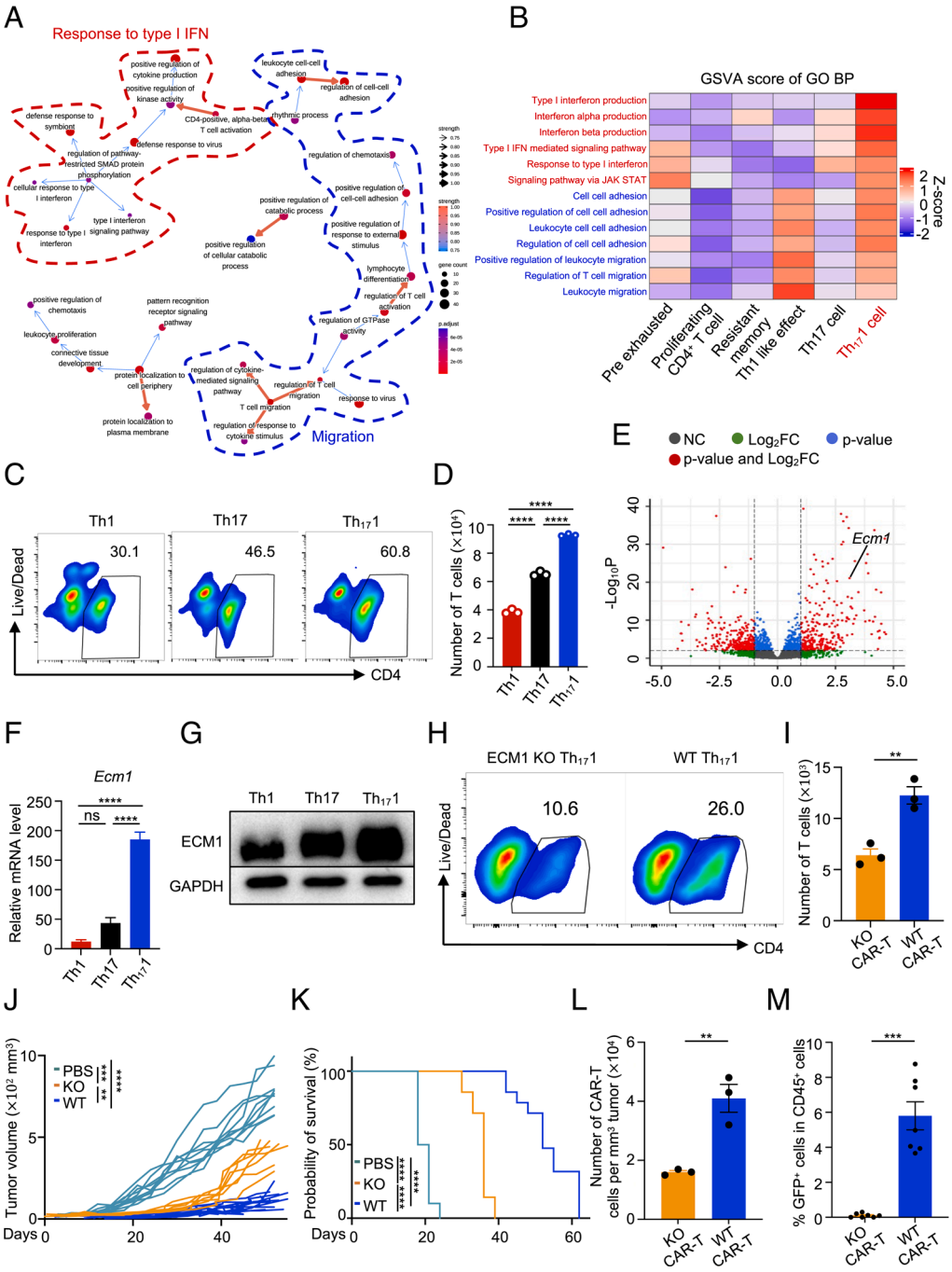

Fig. 5. $Th_{17}1$ cells migrate better in an ECM1-dependent manner. (*A*) CBN plot illustrating gene pathway relationships in $Th_{17}1$ cells. (*B*) GSEA of scRNA-seq data (Fig. 1) showing cellular characteristics. (*C* and *D*) Flow cytometry analysis of migrated T cells in transwell assays with B16 tumor cells after 12 h. (*E*) Volcano plot from RNA-seq comparing gene expression between $Th_{17}1$ and Th1 cells. (*F*) qPCR analysis of *Ecm1* expression in Th1, Th17, and $Th_{17}1$ cells. (*G*) Western blot of ECM1 expression in differentiated cells on day 9. (*H* and *I*) Migration assay comparing ECM1 KO and WT $Th_{17}1$ cells. (*J* and *K*) Tumor growth and survival in MB49-CD19 tumor-bearing mice treated with ECM1 KO or WT $Th_{17}1$ CAR-T cells (n = 7 to 11). (*L*) Tumor infiltration of CAR-T cells on day 7 posttransfer (n = 3). (*M*) GFP^+ CAR-T cells in blood on day 14. Data represent mean ± SEM. $^*P < 0.05$; $^{**}P < 0.01$; $^{***}P < 0.001$; $^{****}P < 0.0001$.

exhaustion and apoptosis in $Th_{17}1$ cells (Fig. 6 *E* and *F* and *SI Appendix*, Fig. S7 *F* and *G*), highlighting that IRF7-mediated type I interferon signature accounts for the less exhausted status of $Th_{17}1$ cells.

Notably, in an experimental autoimmune encephalomyelitis model (36), scRNA-seq data revealed concurrent high expression of *Irf7* and *Ecm1* in IFN-γ^+ IL-17^+ Th1-like Th17 cells (*SI Appendix*, Fig. S7 *H–J*). This observation prompted us to investigate whether IRF7 directly regulates ECM1 expression. We identified a conserved IRF7 binding site in the ECM1 regulatory region (Fig. 6*G*). Chromatin immunoprecipitation result showed a direct binding of IRF7 to the ECM1 promoter (Fig. 6*H*). Consistently, knockdown of IRF7 decreased ECM1 expression (Fig. 6*I*) and reduced migration in $Th_{17}1$ cells (Fig. 6*J*).

In summary, above findings revealed a pivotal role in $Th_{17}1$ cells for maintaining the unique phenotype including early exhausted state and ECM1-dependent migration.

IFN-γ Endows $Th_{17}1$ Cells a Unique Type I IFN Response–Related Transcriptional Pattern by Up-Regulating IRF7. Given IRF7 expression typically remains low in Th1 cells (37), we wondered what signals up-regulated IRF7 expression in $Th_{17}1$ cells. Notably,

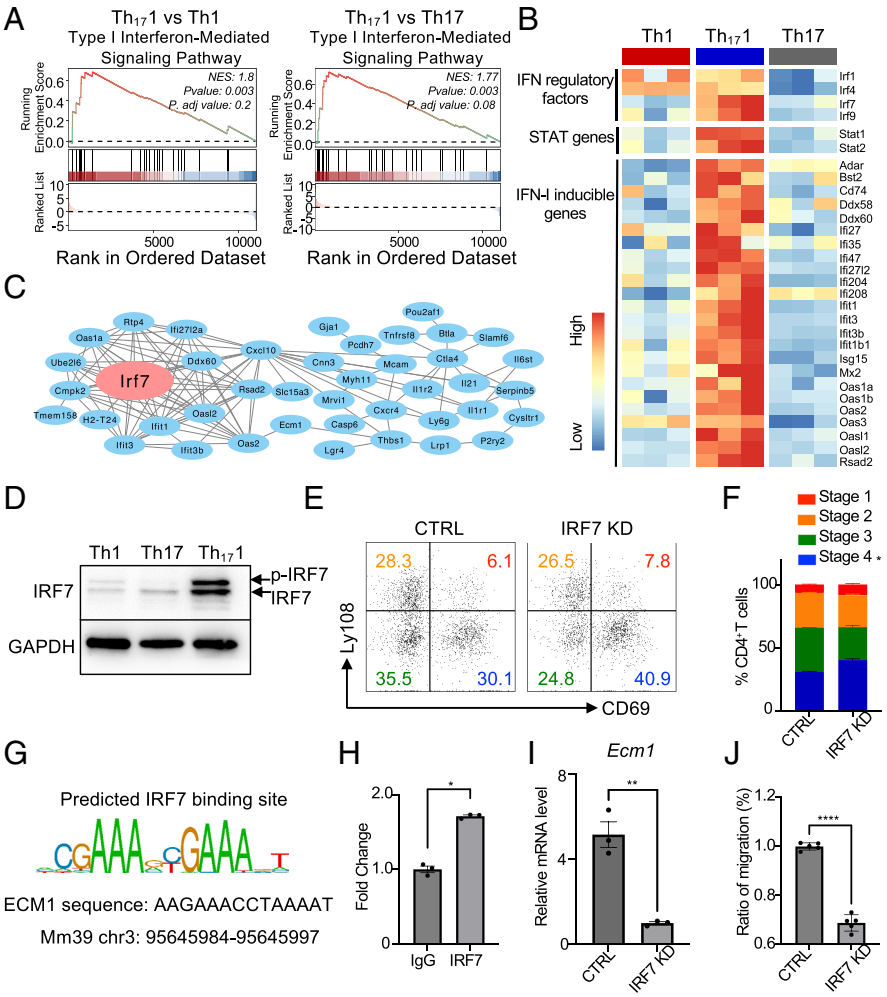

Fig. 6. IRF7-mediated type I IFN response network accounts for the early exhausted feature and ECM1 upregulation in $Th_{17}1$ cells. (*A*) Changes in pathways ($Th_{17}1$ vs. Th1 and $Th_{17}1$ vs. Th17) analyzed by GSVA of bulk RNA-seq data. (*B*) Heatmap of type I interferon response genes in Th1, Th17, and $Th_{17}1$ cells. (*C*) PPI network of up-regulated genes in $Th_{17}1$ cells. (*D*) IRF7 protein expression in differentiated cells (day 9). (*E* and *F*) Ly108 and CD69 staining in control and IRF7 knockdown $Th_{17}1$ cells. (*G*) Predicted IRF7 binding site on *Ecm1* gene. (*H*) ChIP analysis of the binding of IRF7 to the *Ecm1* gene in $Th_{17}1$ cells. *Ecm1* mRNA expression (*I*) and migration assay (*J*) for the $Th_{17}1$ cells after *Irf7* knockdown. Experiments were performed with at least three biological replicates with at least two independent experiments except bioinformatics data. Data are presented as mean ± SEM. $^*P < 0.05$; $^{**}P < 0.01$; $^{***}P < 0.001$; $^{****}P < 0.0001$.

the master regulator, T-bet, and the effector cytokine, IFN-γ, associated with Th1 cells, which typically curtails the type I IFN transcriptome, are found to be compromised in $Th_{17}1$ cells (Fig. 7 *A* and *B*). GSEA demonstrated an increased janus kinase-signal transducer and activator of transcription (JAK-STAT) pathway in $Th_{17}1$ cells compared to Th1 and Th17 cells (Fig. 7*C*). This finding is supported by augmented expression of STAT1 at both mRNA and protein levels (Fig. 7*D* and *SI Appendix*, Fig. S7*A*). Furthermore, phosphorylation of STAT1 is increased in $Th_{17}1$ cells (Fig. 7*D*). These results hint that T cell–derived type I interferons may account for the upregulation of IRF7. However, we were unable to detect any expression of type I interferons in Th1, Th17, or $Th_{17}1$ cells (*SI Appendix*, Table S4), which may explain the barely detectable level of STAT2 phosphorylation (*SI Appendix*, Fig. S7*K*). Importantly, blocking type I interferon signaling by IFNAR1 antibody (αIFNAR1) have no effect on the expression of *Irf7* and *Isg15* (Fig. 7 *E* and *F*). Unexpectedly, IFN-γ neutralization (αIFN-γ) significantly reduces the expression of *Irf7* and *Isg15* (Fig. 7 *E* and *F*).

Blocking IFN-γ inhibited STAT1 phosphorylation and reduced total and phosphorylated IRF7 levels (Fig. 7*G*). Additionally, IFN-γ blockade increased $Th_{17}1$ cell exhaustion (Fig. 7 *H* and *I*) and decreased ECM1 expression, which correlated with reduced migratory capacity (Fig. 7*J*). To verify whether STAT1 mediates the effect of IFN-γ on the phenotype of $Th_{17}1$ cells, we employed a STAT1 inhibitor, fludarabine. STAT1 inhibition promoted $Th_{17}1$ cell exhaustion (Fig. 7 *K* and *L*) and decreased their migration (Fig. 7*M*). Western blot results demonstrated that the STAT1 inhibitor blocked its phosphorylation, along with the suppressed expression of IRF7 and ECM1 (Fig. 7*N*), consistent with the results of IFN-γ blocking (Fig. 7*G*).

Additionally, using TCGA bulk RNA-seq and scRNA-seq data, we identified a positive correlation between IFN-γ and IRF7 in $Th_{17}1$ cells from cancer patients (*SI Appendix*, Fig. S8). To experimentally validate this, we analyzed peripheral blood mononuclear cell (PBMC) samples from bladder cancer patients and confirmed the presence of $Th_{17}1$ cells (Fig. 7*O*), which expressed significantly higher levels of IRF7 compared to IFN-γ^+ Th1 and IL-17A$^+$ Th17 cells (Fig. 7 *P* and *Q*). These results strongly indicate that the induction and activation of IRF7 in $Th_{17}1$ cells are primarily driven by the IFN-γ-activated STAT1 signaling pathway.

Th17 Origin Confers Unique Characteristics to $Th_{17}1$ Cells. Th1 and $Th_{17}1$ cells both produce IFN-γ, but only $Th_{17}1$ cells can initiate the IFN-γ-driven IRF7-mediated responses. T-bet (*Tbx21*), which is highly expressed in Th1 cells, is known to inhibit type I interferon signaling (37). Thus, we wondered whether the

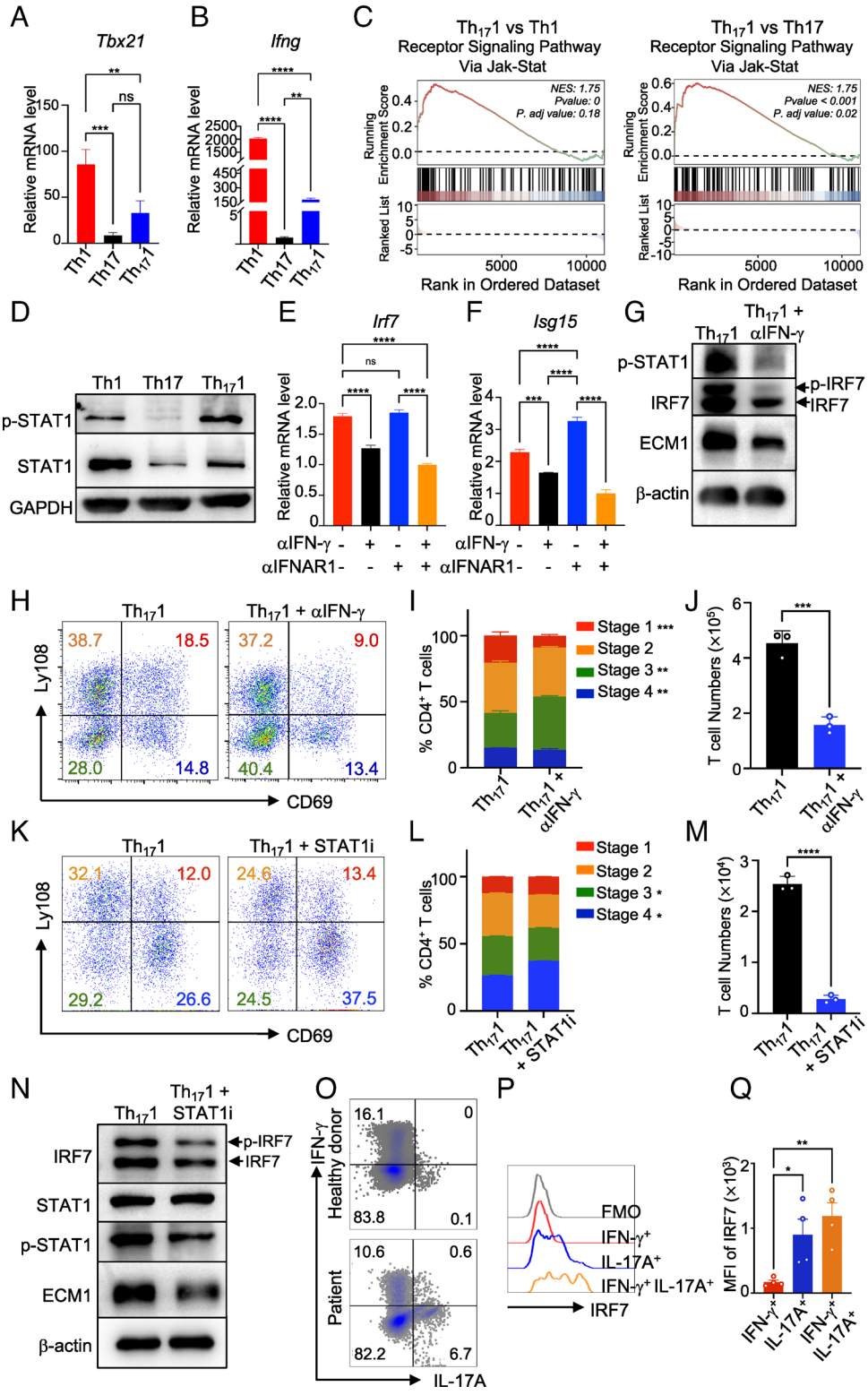

Fig. 7. IFN-γ endows $Th_{17}1$ cells a unique type I IFN response–related transcriptional pattern by up-regulating IRF7. (*A* and *B*) Relative mRNA expression of *Tbx21* and *Ifng* in in vitro-differentiated Th1, Th17, and $Th_{17}1$ cells. (*C*) GSEA of the pathway receptor signaling pathway via JAK-STAT utilizing bulk RNA-seq results from Th1, Th17, and $Th_{17}1$ cells. (*D*) Western blot analysis of STAT1 expression and phosphorylation on day 9. (*E* and *F*) mRNA expression of *Irf7* and *Isg15* under control, IFN-γ blockade (αIFN-γ), IFNAR1 blockade (αIFANR1), and combined IFN-γ/IFNAR1 blockade. (*G*) Western blot analysis of p-STAT1, IRF7, and ECM1 in $Th_{17}1$ cells with or without IFN-γ blockade. (*H–J*) Exhaustion status and migration ability of $Th_{17}1$ cells with or without IFN-γ blockade. (*K–N*) Effects of STAT1 inhibitor on exhaustion status, migration ability, and expression of p-STAT1, IRF7, and ECM1 in $Th_{17}1$ cells. (*O*) Flow cytometry analysis of IFN-γ^+, IL-17A$^+$, and IFN-γ^+IL-17A$^+$ T cells in the blood of healthy donors and bladder cancer patients. (*P* and *Q*) IRF7 expression and mean fluorescence intensity (MFI) in IFN-γ^+, IL-17A$^+$, and IFN-γ^+IL-17A$^+$ T cells. Data are presented as mean ± SEM. $^{**}P < 0.01$; $^{***}P < 0.001$; $^{****}P < 0.0001$.

lack of IRF7-dependent responses in Th1 cells could be attributed to the transcriptional repression of T-bet. First, ChIP-seq data demonstrated that T-bet directly bound to the regulatory regions of *Irf7*, as well as other interferon-responsive genes including *Isg15*, and *Oasl2* (*SI Appendix*, Fig. S9*A*). Moreover, T-bet deficiency in CD4$^+$ T cells led to an increased level of histone H3K27

acetylation at *Irf7, Isg15*, and *Oasl2* loci (*SI Appendix*, Fig. S9*A*). Accordingly, under IFN-γ stimulation, T-bet-KO $CD4^+$ T cells express significantly higher levels of *Irf7, Isg15*, and *Oasl2* when compared to WT $CD4^+$ T cells (*SI Appendix*, Fig. S9*B*), indicating that T-bet acts as a direct transcriptional repressor of the ISGs.

We further explored whether differential T-bet levels underlay the distinct ISG expression patterns among Th1 and Th17 cells. In Th1 cells, higher expression of *Tbx21* led to a stronger repression of *Irf7* even in the high level of IFN-γ expression (*SI Appendix*, Fig. S9*C*). In contrast, the lower T-bet levels in Th17 cells (precursors of $Th_{17}1$ cells) facilitated greater chromatin accessibility and enhanced ISG expression (*SI Appendix*, Fig. S9*C*). This was further supported by experiments showing that IFN-γ blockade significantly reduced *Irf7* expression in Th17 but not Th1 cells, highlighting the role of basal T-bet levels in modulating IFN-γ responsiveness and IRF7 activation (*SI Appendix*, Fig. S9 *D–F*). These findings suggest that Th17-derived cells, like $Th_{17}1$ cells, are possibly more prone to up-regulate ISGs upon exposure to IFN-γ.

To determine whether $Th_{17}1$ cells represent a unique subset, we conducted a comparative analysis with previously reported hybrid Th1/Th17 cells (19). Our results indicate that $Th_{17}1$ cells have distinct transcriptional profiles, with elevated expression of stemness-related markers (*SI Appendix*, Fig. S10 *A* and *B*). Furthermore, $Th_{17}1$ cells displayed decreased PD-1 expression, confirming the unique attributes of $Th_{17}1$ cells (*SI Appendix*, Fig. S10*C*). To further characterize $Th_{17}1$ cells in relation to other atypical Th1 subsets, we differentiated hybrid Th1/Th17 cells, pathogenic $Th_{17}1$ cells ($pTh_{17}1$), and $Th_{17}1$ cells and analyzed their phenotypes. Principal component analysis of RNA-seq data from these subsets revealed distinct transcriptional profiles (*SI Appendix*, Fig. S10*D*). Significant differences in global gene expression further confirmed that $Th_{17}1$ cells are distinct from both hybrid Th1/Th17 and $pTh_{17}1$ cells (*SI Appendix*, Fig. S10*E*). While no clear trends emerged in the expression of stemness or exhaustion-related genes (*SI Appendix*, Fig. S10*F*), $Th_{17}1$ cells consistently showed lower PD-1 expression (*SI Appendix*, Fig. S10*G*). Notably, $Th_{17}1$ cells exhibited reduced apoptosis (*SI Appendix*, Fig. S10 *H* and *I*) and enhanced activity in the JAK-STAT and type I interferon pathways (*SI Appendix*, Fig. S10 *J* and *K*). Moreover, $Th_{17}1$ cells were enriched for the cell migration pathway (*SI Appendix*, Fig. S10*L*) with high expression of *Ecm1* (*SI Appendix*, Fig. S10*M*) and demonstrated superior migratory capacity (*SI Appendix*, Fig. S10*N*).

In summary, these findings clearly demonstrate that $Th_{17}1$ cells represent a unique $CD4^+$ T cell subset, characterized by distinct transcriptional profiles, signaling pathways, and functional properties.

Discussion

$IL\text{-}17A^+$ $IFN\text{-}\gamma^+$ T cells, commonly referred to as Th1/Th17 or exTh17 cells or atypical Th1 cells, have been found to be enriched in autoimmune conditions such as colitis, arthritis, and multiple sclerosis (17–19), (38–42). CD161 has been identified as a key marker for distinguishing these Th1/Th17 cells from classic Th1 cells (43, 44). The signaling pathways involving IL-1β, IL-21, and IL-23 are known to play crucial roles in the differentiation of Th17 cells and potentially contribute to the development of $IL\text{-}17A^+$ $IFN\text{-}\gamma^+$ cells (45–48). For example, in Crohn's disease, $CD161^+$ $CD4^+$ T cells in patient tissues express IL-23R and can be induced by IL-23 to coexpress IL-17 and IFN-γ (49). Additionally, the generation of encephalitogenic $IL\text{-}17A^+$ $IFN\text{-}\gamma^+$ T cells is dependent on IL-1β signaling (17). Although the specific role of IL-21 in $IL\text{-}17A^+$ $IFN\text{-}\gamma^+$ T cells remains unclear, IL-21 is highly expressed in hybrid Th1/Th17 cells, and our $Th_{17}1$ cells (*SI Appendix*, Fig. S10*A*). While IL-1β, IL-21, and IL-23 do not directly induce IRF7, they may contribute to the proinflammatory and cytokine-rich environment that enhances IRF7 expression through IFN-γ and type I interferon signaling. However, the role of atypical Th1 cells in tumor biology remains unclear. The presence of Th1/Th17 hybrid cells has been reported in human tumors (50, 51). Chatterjee et al. reported that hybrid murine Th1/Th17 cells, generated under Th1 and Th17 mixed culture condition, have enhanced antitumor ability (19). Our bioinformatic analysis suggests that in vivo-differentiated $CD4^+$ T cells coexpressing IFN-γ and IL-17 may have the ability to suppress tumor growth and benefit patient survival, which emphasizes the important role of IFN-γ and IL-17 coexpressing $CD4^+$ T cells in tumor suppression. However, our study using differentiation trajectory analysis of single cell RNA-seq dataset revealed that $Th_{17}1$ cells, a subset of atypical Th1 cells, are directly differentiated from Th17 cells in vivo. Thus, our procedure to induce $Th_{17}1$ cell differentiation may represent a more accurate reflection of their in vivo counterparts. Transcriptional and functional studies further confirmed that $Th_{17}1$ cells are distinct from other atypical Th1 cells, representing a unique subset with specific functional properties.

The role of T cell intrinsic type I IFN signaling in the antitumor response has been less investigated and remains controversial (33, 52). T cells typically do not express type I interferons due to the strong inhibitory effect of T-bet in type I interferon transcriptome (37). However, CAR-T cells with combined CD28 and 4-1BB expression demonstrated sustained activation of IRF7/IFNβ pathway. Knockdown of IRF7 was shown to impair their antitumor efficacy (52). In contradictory, chronic IRF7-mediated type I IFN production in T cells has been associated with poor CAR T-cells persistence in patients with B cell malignancies (34). It is also reported that type I IFN drives $CD8^+$ T cell exhaustion in an IRF7-dependent manner in the context of chronic LCMV infection and cancers (33), (53). Interestingly, a cluster of $CD4^+$ T cells exhibiting enriched IFN response and less exhaustion in patients with B cell malignancies, suggesting an enhanced IFN response may correlate with decreased T cell exhaustion (34). Our study identifies a type I IFN-related transcriptome in $Th_{17}1$ cells, characterized by elevated IRF7 expression and ISGs along with a less exhausted status. Inhibition of IRF7 expression significantly decreases the expression of ISGs and exacerbated the exhaustion of $Th_{17}1$ cells, demonstrating that the IRF7-mediated type I IFN response endows $Th_{17}1$ cells with a less exhausted status.

It is intriguing to understand how $Th_{17}1$ cells acquire the IRF7-mediated type I IFN response signature. IFN-γ, primarily produced by activated T cells and NK cells, plays a profound role in modulating T cell behavior (54). IFN-γ works by binding to IFNGR, activating STAT1, and inducing T-bet expression (54). In Th1 cells, T-bet strongly suppresses IRF7 and the type I IFN response. However, $Th_{17}1$ cell's unique differentiation trajectory allows for some degree of type I IFN transcriptome induction during the initial Th17 differentiation stage, as indicated by intermediate IRF7 expression in Th17 cells compared with Th1 and $Th_{17}1$ cells. When $Th_{17}1$ cells differentiate under Th1 condition, induced by IL-12, they exhibit compromised T-bet and IFN-γ expression. Despite this, the lower T-bet levels primarily function to promote IFN-γ transcription without fully repressing IRF7 and ISGs expression. IFN-γ, in turn, activates STAT1, up-regulates IRF7, and establishes a T cell intrinsic Type I interferon responsive network. The association of IRF7 with both early exhaustion and ECM1-dependent migration underscores its central role in shaping $Th_{17}1$ cells function.

In summary, $Th_{17}1$ cells offer a unique convergence of attributes, including reduced exhaustion, enhanced migration, and better antitumor activity, collectively addressing critical limitations in current immunotherapeutic approaches. Harnessing the potential of $Th_{17}1$ cells and exploring the role of T cell intrinsic type I IFN signaling could pave the way for strategies to combat solid tumors, providing renewed hope for improved clinical outcomes in cancer immunotherapy.

Methods and Materials

Mice and cell lines, in vitro-polarizing conditions for Th17, Th1, $Th_{17}1$, and $Th_{1}17$ cells, $Th_{17}1$ lineage tracing assay, viral production and transduction, induction of B16 lung prophylactic model, tumor inoculation and therapy, isolation T cells from tumors, lymph nodes and spleens, T cell transwell assay, flow cytometry, seahorse, scRNA-seq data analysis, TCGA survival analysis, bulk RNA-seq, publicly available RNA-seq data, ChIP-seq data and ATAC-seq data analysis, real-time PCR, plasmids, ChIP assay, western blot, $CD8^+$ T Cell depletion, and statistical analysis can be found in *SI Appendix, Materials and Methods*. All animal experiments were conducted according to approved protocols by the animal care and use committee of Southern Medical University. Experiments using human PBMCs were performed according to the guidelines of the ethics committee at the Zhujiang Hospital, Southern Medical University.

Data, Materials, and Software Availability. RNA-seq data generated in this study can be accessed at GSE244717 (55) and GSE276409 (56). All other data are included in the article and/or *SI Appendix*.

ACKNOWLEDGMENTS. This study was financially supported by National Natural Science Foundation of China (82172709, 82372775, 82373236, 82171725, and 82090022), Guangdong Basic and Applied Basic Research Foundation (2021A1515012540, 2023A1515012514, and 2023A1515010257).

Author affiliations: [a]Department of Biochemistry and Molecular Biology, School of Basic Medical Sciences, Guangdong Provincial Key Laboratory of Single Cell Technology and Application, Southern Medical University, Guangzhou, Guangdong 510515, China; [b]Division of Nephrology, State Key Laboratory of Organ Failure Research, National Clinical Research Center of Kidney Disease, Guangdong Provincial Institute of Nephrology, Guangdong Provincial Key Laboratory of Renal Failure Research, Nanfang Hospital, Southern Medical University, Guangzhou 510515, China; [c]Department of Urology, Zhujiang Hospital, Southern Medical University, Guangzhou 510280, China; and [d]Guangdong Provincial Key Laboratory of Medical Molecular Diagnostics, Guangdong Medical University, Dongguan 523808, China

1. M. Ruella, M. Kalos, Adoptive immunotherapy for cancer. *Immunol. Rev.* **257**, 14–38 (2014).
2. J. Alfred Witjes *et al.*, Updated 2016 EAU guidelines on muscle-invasive and metastatic bladder cancer. *Eur. Urol.* **71**, 462–475 (2017).
3. N. P. Restifo, M. E. Dudley, S. A. Rosenberg, Adoptive immunotherapy for cancer: Harnessing the T cell response. *Nat. Rev. Immunol.* **12**, 269–281 (2012).
4. S. L. Maude *et al.*, Chimeric antigen receptor T cells for sustained remissions in leukemia. *N. Engl. J. Med.* **371**, 1507–1517 (2014).
5. J. J. Peng, L. Wang, Z. Li, C. L. Ku, P. C. Ho, Metabolic challenges and interventions in CAR T cell therapy. *Sci. Immunol.* **8**, eabq3016 (2023).
6. S. Rafiq, C. S. Hackett, R. J. Brentjens, Engineering strategies to overcome the current roadblocks in CAR T cell therapy. *Nat. Rev. Clin. Oncol.* **17**, 147–167 (2020).
7. H. Kagamu *et al.*, Single-cell analysis reveals a CD4+ T-cell cluster that correlates with PD-1 blockade efficacy. *Cancer Res.* **82**, 4641–4653 (2022).
8. E. Cano-Gamez *et al.*, Single-cell transcriptomics identifies an effectorness gradient shaping the response of CD4(+) T cells to cytokines. *Nat. Commun.* **11**, 1801 (2020).
9. L. Zheng *et al.*, Pan-cancer single-cell landscape of tumor-infiltrating T cells. *Science* **374**, abe6474 (2021).
10. B. Kruse *et al.*, CD4(+) T cell-induced inflammatory cell death controls immune-evasive tumours. *Nature* **618**, 1033–1040 (2023).
11. G. Oliveira *et al.*, Landscape of helper and regulatory antitumour CD4(+) T cells in melanoma. *Nature* **605**, 532–538 (2022).
12. R. E. Tay, E. K. Richardson, H. C. Toh, Revisiting the role of CD4(+) T cells in cancer immunotherapy-new insights into old paradigms. *Cancer Gene Ther.* **28**, 5–17 (2021).
13. A. Cachot *et al.*, Tumor-specific cytolytic CD4 T cells mediate immunity against human cancer. *Sci. Adv.* **7**, 9 (2021).
14. D. Y. Oh *et al.*, Intratumoral CD4(+) T cells mediate anti-tumor cytotoxicity in human bladder cancer. *Cell* **181**, 1612–1625 (2020).
15. I. Taniuchi, CD4 helper and CD8 cytotoxic T cell differentiation. *Annu. Rev. Immunol.* **36**, 579–601 (2018).
16. W. Zou, N. P. Restifo, T(H)17 cells in tumour immunity and immunotherapy. *Nat. Rev. Immunol.* **10**, 248–256 (2010).
17. F. Ronchi *et al.*, Experimental priming of encephalitogenic Th1/Th17 cells requires pertussis toxin-driven IL-1beta production by myeloid cells. *Nat. Commun.* **7**, 11541 (2016).
18. S. N. Harbour, C. L. Maynard, C. L. Zindl, T. R. Schoeb, C. T. Weaver, Th17 cells give rise to Th1 cells that are required for the pathogenesis of colitis. *Proc. Natl. Acad. Sci. U.S.A.* **112**, 7061–7066 (2015).
19. S. Chatterjee *et al.*, CD38-NAD(+) axis regulates immunotherapeutic anti-tumor T cell response. *Cell Metab.* **27**, 85–100 (2018).
20. C. Chen *et al.*, Vitamin B5 rewires Th17 cell metabolism via impeding PKM2 nuclear translocation. *Cell Rep.* **41**, 111741 (2022).
21. S. Ma, Y. Ming, J. Wu, G. Cui, Cellular metabolism regulates the differentiation and function of T-cell subsets. *Cell Mol. Immunol.* **21**, 419–435 (2024).
22. I. Y. Jung *et al.*, Type I interferon signaling via the EGR2 transcriptional regulator potentiates CAR T cell-intrinsic dysfunction. *Cancer Discov.* **13**, 1636–1655 (2023).
23. H. Fu *et al.*, The glucose transporter 2 regulates CD8(+) T cell function via environment sensing. *Nat. Metab.* **5**, 1969–1985 (2023).
24. S. K. Vodnala *et al.*, T cell stemness and dysfunction in tumors are triggered by a common mechanism. *Science* **363**, eaau0135 (2019).
25. X. Ma *et al.*, Cholesterol induces CD8(+) T cell exhaustion in the tumor microenvironment. *Cell Metab.* **30**, 143–156.e5 (2019).
26. D. Geng *et al.*, When Toll-like receptor and T-cell receptor signals collide: A mechanism for enhanced CD8 T-cell effector function. *Blood* **116**, 3494–3504 (2010).
27. S. T. Ju, H. Cui, D. J. Panka, R. Ettinger, A. Marshak-Rothstein, Participation of target Fas protein in apoptosis pathway induced by CD4+ Th1 and CD8+ cytotoxic T cells. *Proc. Natl. Acad. Sci. U.S.A.* **91**, 4185–4189 (1994).
28. R. I. K. Geltink, R. L. Kyle, E. L. Pearce, Unraveling the complex interplay between T cell metabolism and function. *Annu. Rev. Immunol.* **36**, 461–488 (2018).
29. A. Chow, K. Perica, C. A. Klebanoff, J. D. Wolchok, Clinical implications of T cell exhaustion for cancer immunotherapy. *Nat. Rev. Clin. Oncol.* **19**, 775–790 (2022).
30. J. C. Beltra *et al.*, Developmental relationships of four exhausted CD8(+) T cell subsets reveals underlying transcriptional and epigenetic landscape control mechanisms. *Immunity* **52**, 825–841 e828 (2020).
31. N. Sato, Y. Tamada, G. Yu, Y. Okuno, CBNplot: Bayesian network plots for enrichment analysis. *Bioinformatics* **38**, 2959–2960 (2022).
32. Z. Li *et al.*, ECM1 controls T(H)2 cell egress from lymph nodes through re-expression of S1P(1). *Nat. Immunol.* **12**, 178–185 (2011).
33. T. Wu *et al.*, The TCF1-Bcl6 axis counteracts type I interferon to repress exhaustion and maintain T cell stemness. *Sci. Immunol.* **1**, eaai8593 (2016).
34. G. M. Chen *et al.*, Integrative bulk and single-cell profiling of premanufacture T-cell populations reveals factors mediating long-term persistence of CAR T-cell therapy. *Cancer Discov.* **11**, 2186–2199 (2021).
35. R. Colina *et al.*, Translational control of the innate immune response through IRF-7. *Nature* **452**, 323–328 (2008).
36. P. W. F. Karmaus *et al.*, Metabolic heterogeneity underlies reciprocal fates of T(H)17 cell stemness and plasticity. *Nature* **565**, 101–105 (2019).
37. S. Iwata *et al.*, The transcription factor T-bet limits amplification of type I IFN transcriptome and circuitry in T helper 1 cells. *Immunity* **46**, 983–991.e4 (2017).
38. J. van Langelaar *et al.*, T helper 17.1 cells associate with multiple sclerosis disease activity: Perspectives for early intervention. *Brain* **141**, 1334–1349 (2018).
39. V. Friedrich *et al.*, Helicobacter hepaticus is required for immune targeting of bacterial heat shock protein 60 and fatal colitis in mice. *Gut Microbes* **13**, 1–20 (2021).
40. F. Annunziato *et al.*, Phenotypic and functional features of human Th17 cells. *J. Exp. Med.* **204**, 1849–1861 (2007).
41. L. Maggi *et al.*, Brief report: Etanercept inhibits the tumor necrosis factor alpha-driven shift of Th17 lymphocytes toward a nonclassic Th1 phenotype in juvenile idiopathic arthritis. *Arthritis Rheumatol.* **66**, 1372–1377 (2014).
42. K. Nistala *et al.*, Th17 plasticity in human autoimmune arthritis is driven by the inflammatory environment. *Proc. Natl. Acad. Sci. U.S.A.* **107**, 14751–14756 (2010).
43. L. Maggi *et al.*, Distinctive features of classic and nonclassic (Th17 derived) human Th1 cells. *Eur. J. Immunol.* **42**, 3180–3188 (2012).
44. S. A. Basdeo *et al.*, Ex-Th17 (Nonclassical Th1) cells are functionally distinct from classical Th1 and Th17 cells and are not constrained by regulatory T cells. *J. Immunol.* **198**, 2249–2259 (2017).
45. C. Sutton, C. Brereton, B. Keogh, K. H. Mills, E. C. Lavelle, A crucial role for interleukin (IL)-1 in the induction of IL-17-producing T cells that mediate autoimmune encephalomyelitis. *J. Exp. Med.* **203**, 1685–1691 (2006).
46. T. Korn *et al.*, IL-21 initiates an alternative pathway to induce proinflammatory T(H)17 cells. *Nature* **448**, 484–487 (2007).
47. L. Yang *et al.*, IL-21 and TGF-beta are required for differentiation of human T(H)17 cells. *Nature* **454**, 350–352 (2008).
48. S. L. Gaffen, R. Jain, A. V. Garg, D. J. Cua, The IL-23-IL-17 immune axis: From mechanisms to therapeutic testing. *Nat. Rev. Immunol.* **14**, 585–600 (2014).
49. M. A. Kleinschek *et al.*, Circulating and gut-resident human Th17 cells express CD161 and promote intestinal inflammation. *J. Exp. Med.* **206**, 525–534 (2009).
50. I. Kryczek *et al.*, Phenotype, distribution, generation, and functional and clinical relevance of Th17 cells in the human tumor environments. *Blood* **114**, 1141–1149 (2009).
51. A. Hamai *et al.*, Human T(H)17 immune cells specific for the tumor antigen MAGE-A3 convert to IFN-gamma-secreting cells as they differentiate into effector T cells in vivo. *Cancer Res.* **72**, 1059–1063 (2012).

52. Z. Zhao *et al.*, Structural design of engineered costimulation determines tumor rejection kinetics and persistence of CAR T cells. *Cancer Cell* **28**, 415–428 (2015).
53. M. Y. Kasmani *et al.*, Clonal lineage tracing reveals mechanisms skewing CD8+ T cell fate decisions in chronic infection. *J. Exp. Med.* **220**, e20220679 (2023).
54. F. Castro, A. P. Cardoso, R. M. Goncalves, K. Serre, M. J. Oliveira, Interferon-gamma at the crossroads of tumor immune surveillance or evasion. *Front. Immunol.* **9**, 847 (2018).
55. Z. Chen *et al.*, Th17-derived Th1 cells resemble progenitor exhausted CD4+ T cells and exhibit augmented anti-tumor efficacy. Gene Expression Omnibus. https://www.ncbi.nlm.nih.gov/geo/query/acc.cgi?acc=GSE244717. Deposited 1 June 2024.
56. X. Lei *et al.*, The antitumor function of Th17-derived Th1 cell is better than traditional Th1 and Th17 cells. Gene Expression Omnibus. https://www.ncbi.nlm.nih.gov/geo/query/acc.cgi?acc=GSE276409. Deposited 31 October 2024.